Jamming and Crystallization of Polymeric Micelles

Taco Nicolai* and Fabrice Laflèche

Polymères, Colloïdes, Interfaces, UMR CNRS, Université du Maine, 72085 Le Mans Cedex 9, France

Alain Gibaud

Laboratoire de Physique de l'Etat Condensé, UMR CNRS, Université du Maine, 72085 Le Mans Cedex 9, France

Received May 7, 2004; Revised Manuscript Received August 4, 2004

ABSTRACT: The dynamic mechanical and structural properties of polymeric micelles, formed by hydrophobically end-capped poly(ethylene oxide) (PEO) in water, were studied as a function of concentration and temperature. A discontinuous liquid−solid transition is observed during a temperature quench at a critical temperature (T_c) that increases with increasing micelle concentration. The transition is fast except after a quench to a temperature just below T_c where it may take as long as 24 h. A body-centered-cubic phase is formed relatively quickly after the liquid−solid transition, i.e., in the jammed system. The fraction of crystalline material in the solid increases with increasing concentration or decreasing temperature. The viscosity of the liquid phase has a power law concentration dependence similar to that of polymer stars with a relatively small numbers of arms.

Introduction

Polymers containing a single small insoluble group form spherical polymeric micelles in solution above a critical association concentration (CAC). Important examples of water-soluble polymeric micelles are those based on poly(ethylene oxide) (PEO) chains. Polymeric micelles formed by PEO with various hydrophobic groups such as poly(propylene oxide) (Pluronics) and poly(butylene oxide) have been studied extensively.[1]

Scattering experiments have shown that these systems form a cubic crystal phase above a certain concentration. At lower concentrations the interparticle structure factor can be reasonably well described in terms of models developed for hard spheres. The mechanical properties are characterized by a transition from a liquid to a solid behavior over a very narrow concentration range. The solid is sometimes preceded by a range of concentrations in which a so-called soft solid is formed with a lower shear modulus and a smaller yield stress.

The transition to the solid behavior is simultaneous with the appearance of a crystal phase, and it is generally agreed that the solid behavior is caused by jamming of close-packed micelles. The concentration at which the liquid−solid transition occurs increases with increasing temperature because excluded-volume interaction between PEO segments decreases.

The origin of the soft solid is less clear. One possibility is that it is caused by attractive interaction between the micelles which leads to aggregation and percolation at concentrations below close packing.[2] However, the attraction must not be very strong otherwise the system phase separates. Percolation and phase separation was observed, and semiquantitatively described, for polymeric micelles than contain bridging chains.[3] In this case the soft solid is more like a very viscous liquid because the bonds between the micelles that form the system spanning network are reversible. Another proposal to explain the soft solid is that it is a system in which only a fraction of the micelles are crystalline dispersed as crystal grains.[4]

Here we present a study of PEO end-capped with an alkyl group in aqueous solution. This system forms polymeric micelles with an association number of 26 almost independent of the temperature between 20 and 70 °C at least at concentrations below 100 g/L.[3] PEO functionalized at both ends with alkyl groups have been studied extensively for their associative properties.[3,5−14] Single end-capped chains have been less studied. The objective of this work is to compare the mechanical properties as a function of temperature and concentration with the structural changes observed by scattering techniques.

Experimental Section

Materials. PEO end-capped with octadecyl was purchased from Aldrich (Brij700). The weight-average molar mass, M_w = 4.0 kg/mol (about 90 ethylene oxide segments), and polydispersity index, M_w/M_n = 1.05, were determined using size exclusion chromatography and static light scattering. Clear solutions were obtained in "Millipore" water after heating at 80 °C and agitating for about 15 min. The concentrations were obtained by weight and are expressed in gram per liter, since the density of the solutions is very close to 1 kg/L over the whole concentration range.

Methods. Dynamic mechanical measurements were done on a stress-controlled rheometer (AR1000, TA Instruments) using a cone−plate geometry (diameter 4 cm; angle 0.58°). The temperature was controlled using a Peltier system. Solvent evaporation was avoided by covering the geometry with a mineral oil. The stress was chosen low enough to measure a linear viscoelastic response. The viscosities of more dilute systems were determined in flow experiments at low shear rate using a Low Shear 40 (Contraves) rheometer with Couette geometry.

Small-angle X-ray scattering (SAXS) experiments were done at the X21 beamline at the NSLS (Brookhaven, New York) with a pinhole collimation and a Mar CCD detector. Samples were inserted either in capillaries or in flat cells between capton windows. The samples were placed in a heating unit with a temperature control within 1 °C.

* Corresponding author: e-mail Taco.Nicolai@univ-lemans.fr.

10.1021/ma049101y CCC: $27.50
Published on Web 09/21/2004

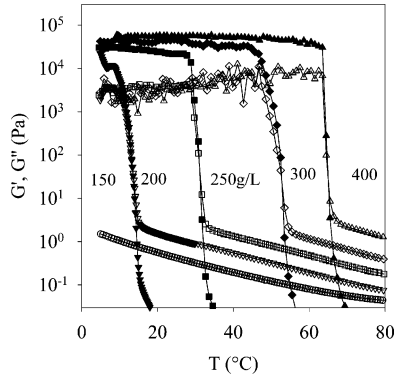

Figure 1. Temperature dependence of the loss (open symbols) and the storage (closed symbols) shear modulus at a frequency 1 Hz. The temperature was decreased at a rate of 5 °C/min.

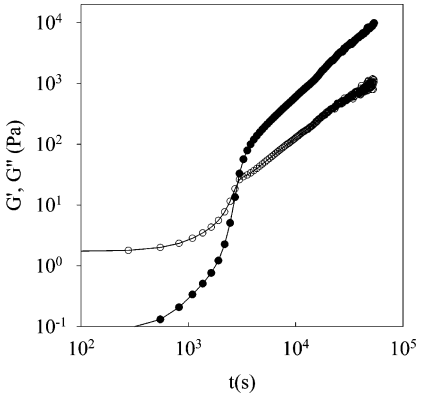

Figure 2. Time dependence of the loss (open symbols) and the storage (closed symbols) shear modulus at a frequency 1 Hz close to the liquid−solid transition (225 g/L, 37 °C).

Results

Dynamic Mechanical Properties. Figure 1 shows the effect of cooling on the loss and storage shear modulus for solutions of PEO chains end-capped with octadecyl at different concentrations. There is a very dramatic increase of both G' and G'' at a critical temperature (T_c) that increases with increasing concentration. The transition is directly between a liquid and a solid behavior, and for this system no intermediate so-called soft solid was observed.

The temperature dependence of the moduli at temperatures much larger or much smaller than T_c is independent of the cooling rate. However, the crossover temperature depends on the rate of the temperature ramp and is different for cooling and heating. The reason is, of course, that the liquid−solid transition is not instantaneous. Far from T_c the transition is very rapid, but it becomes slower closer to T_c. In fact, within a degree or two of T_c the transition becomes extremely slow. This is illustrated for one sample in Figure 2, where we show the time dependence of G' and G'' at a fixed temperature close to T_c. For this system the solid is formed only after many hours. At no temperature did we observe a stable intermediate behavior between the solid and the liquid state, i.e., slowly flowing systems with a viscosity larger than 0.3 Pa s.

We determined the frequency dependence of G' and G'' of the systems at different temperatures. For $T > T_c$ we observed $G \propto f^{1}$ and $G' \propto f^{2}$ that is characteristic for liquids. For $T < T_c$, G' is almost independent of the frequency over a broad range of frequencies, but there appears to be terminal relaxation at very low frequencies ($f < 10^{-4}$ Hz). However, the relaxation at low frequencies is sensitive to the applied stress even at the lowest stress where the deformation was still measurable with some accuracy; the lower is the applied stress, the slower is the terminal relaxation. The flow rate decreases with decreasing shear stress, and a yield stress was not observed. The steady shear viscosity increased with decreasing shear stress down to flow rates as low as 10^{-3} s^{-1}.

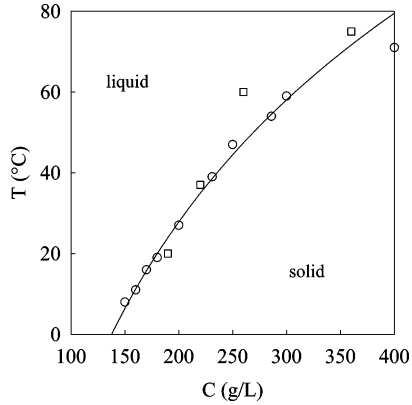

Figure 3. Liquid−solid state diagram. The circles indicate T_c as a function of the concentration. The squares indicate the temperatures where the effective volume fraction of the micelles is unity. The solid line is calculated using $0.02 = 3.2 \times 10^{-10} C^{3.9} \exp(-0.063(T_c - 20))$; see text.

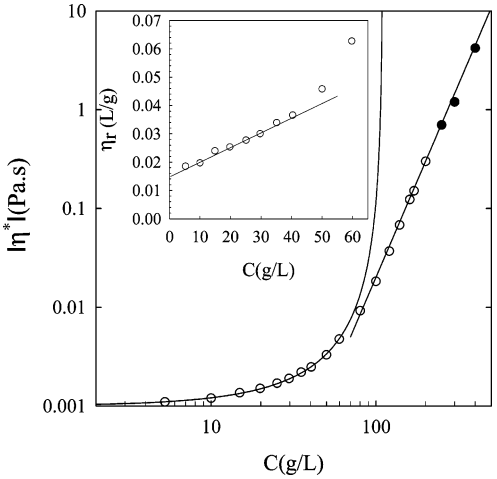

Figure 4. Concentration dependence of the viscosity at 20 °C. The filled points were extrapolated from data at higher temperatures (see Figure 5). The solid line through the data for $C < 80$ g/L represents $\eta = (1 - C/110)^{-2}$. The inset shows the concentration dependence of the intrinsic viscosity. The straight lines represent linear least-squares fits.

However, tilted samples in the solid phase showed no signs of flow over a period of days. The liquid−solid transition can be easily observed manually by tilting the samples. We have determined the freezing temperature as the highest temperature where the liquid system becomes a solid within 12 h and the melting temperature as the lowest temperature where the solid system becomes a liquid within 12 h. The melting and freezing temperatures differ by just 2 or 3 deg, and T_c taken as the average of the two is plotted in Figure 3 as a function of the concentration.

Figure 4 shows the concentration dependence of the viscosity at 20 °C in the liquid phase, i.e., up to $C = 180$ g/L. The intrinsic viscosity, $[\eta]$, and the Huggins coefficient, K_H, are calculated using the initial concen-

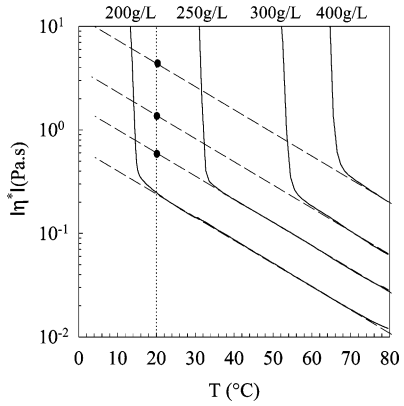

Figure 5. Temperature dependence of the viscosity at different concentrations. The dashed lines describe the temperature dependence in the liquid regime and have the same slope (−0.063). The filled circles indicate viscosities at 20 °C for supercooled solutions at higher concentration obtained by extrapolation of the data at high temperatures.

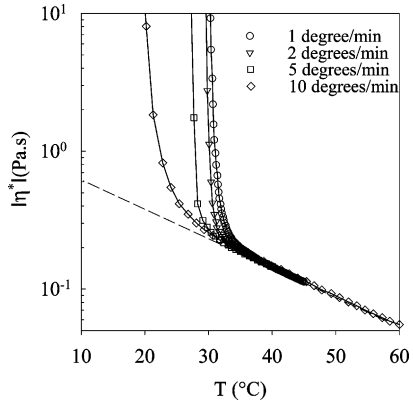

Figure 6. Temperature dependence of the viscosity at 225 g/L at different rates of cooling.

tration dependence of the reduced viscosity ($\eta_r = (\eta - \eta_0)/(C\eta_0)$, with η_0 the solvent viscosity): $\eta_r = [\eta](1 + K_H[\eta]C)$; see inset of Figure 4. A linear least-squares fit yields $[\eta] = 1.6 \times 10^{-2}$ L/g and $K_H = 2.0$.

Figure 5 shows the temperature dependence of the complex viscosity $|\eta^*|$ at 1 Hz during cooling for a number of concentrations. Below the liquid−solid transition $|\eta^*|$ is independent of the frequency, and the storage modulus is negligible so that the complex viscosity may be equated with the viscosity. The viscosity increases exponentially with decreasing temperature ($\eta \propto \exp(-0.063T)$) down until T_c after which $|\eta^*|$ rises rapidly due to the liquid−solid transition. The temperature dependence of the viscosity above T_c is the same at different concentrations and does not depend on the rate of the temperature ramp. The liquid−solid transition appears when the viscosity is about 0.3 Pa s, but the precise value depends on rate of the temperature ramp as is illustrated in Figure 6. Up to the liquid−solid transition $|\eta^*|$ is stable in time, but during the transition the system is out of equilibrium and $|\eta^*|$ increases with time and diverges when the solid is formed.

The data shown in Figures 1 and 5 were obtained at a rate of 5 °C/min. At this cooling rate we can still determine the viscosity at 20 °C for $C = 200$ g/L, while in equilibrium this sample is solid. For higher concentrations we cannot decrease the temperature sufficiently rapidly, but we can obtain the viscosity of the systems in the supercooled state by extrapolating the high-

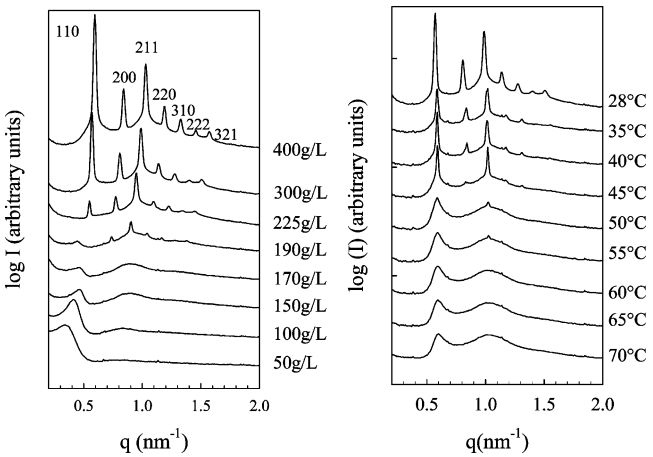

Figure 7. q dependence of the radial averaged scattering intensity as a function of concentration at 28 °C (left) or as a function of temperature at 300 g/L (right). The indexes of the Bragg peaks are indicted in the left panel.

temperature data to 20 °C; see filled circles in Figure 5. These data points have been added in Figure 4 as filled circles. It appears that the viscosity of the supercooled systems follow the same power law concentration dependence as the stable liquids ($\eta = 3.2 \times 10^{-10}C^{3.9}$).

The liquid−solid transition occurs at a constant viscosity (η_c) independent of concentration and temperature. This means that the concentration dependence of T_c can be calculated by combining the power law concentration dependence and the exponential temperature dependence: $\eta_c = 3.2 \times 10^{-10}C^{3.9} \exp(-0.063(T_c - 20))$. The solid line in Figure 3 shows the result of this calculation with $\eta_c = 0.2$ Pa s and compares well with the observed transition except at the highest polymer concentration.

Structural Properties. Figure 7 shows the radial averaged intensity of the systems after equilibrating during at least an hour at a fixed temperature (28 °C) for different concentrations (left panel) or at different temperatures for a fixed concentration (300 g/L) (right panel). Bragg peaks indicating the formation of a crystal structure appear abruptly close to the liquid−solid transition, both when increasing the concentration and when decreasing the temperature. Up to seven peaks can be clearly identified at higher concentrations, and the Bragg peak sequence indexed in the left panel of Figure 7 shows that a body-centered-cubic (bcc) phase is formed with the $Im3m$ symmetry as is generally observed for close-packed polymeric micelles. The relative intensity of the first 110 Bragg peak, at $q \approx 0.6$ nm^{-1}, becomes progressively larger with decreasing temperature and increasing concentration. This effect which is not expected from the $Im3m$ symmetry and is not explained at the moment.

The Bragg peaks becomes stronger with decreasing temperature, but the peak positions do not vary significantly with the temperature. As mentioned above, the association number of the micelles in dilute solutions does not have a significant temperature dependence.[3] We have calculated the dimension of the unit cell a from the peak positions at 28 °C. a varies weakly from 17 nm at 190 g/L to 15 nm at 400 g/L. If all the micelles form one homogeneous cubic phase with a constant association number (p), then $a \propto C^{1/3}$. The experimental concentration dependence of a is weaker, indicating that p increases with C and/or that the system is not homogeneous. It is in any case certain that the average

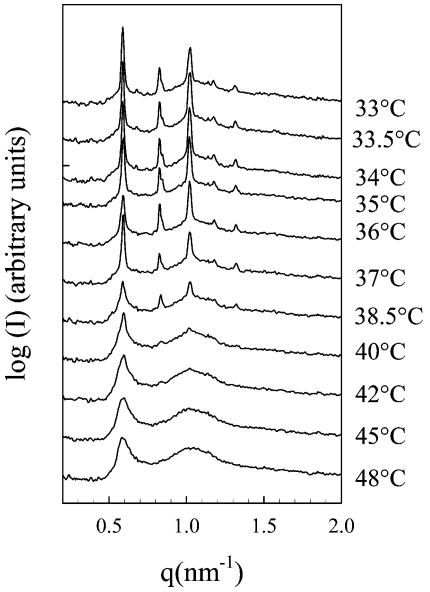

Figure 8. q dependence of the radial averaged scattering intensity at 300 g/L during a temperature quench. The time interval between the spectra is a few minutes.

association number is larger in the concentrated solid phase than in dilute solution where $p = 26$.[3] The association number of micelles in a homogeneous bcc phase is calculated straightforwardly as $p = 0.5N_aCa^3/M$, with N_a Avogadro's number and M the molar mass of the PEO chains (4.0 kg/mol) and accounting for the fact that there are two micelles per unit cell. If it is assumed that all micelles are in the cubic phase, then $p \approx 100$ at $C = 400$ g/L.)

The SAXS setup did not allow for a rapid temperature quench, but spectra taken during a relatively slow quench of a system at 300 g/L are shown in Figure 8. At this concentration T_c is about 55 °C, and the liquid−solid transition occurs close to that temperature during a cooling ramp at 5 °C/min (see Figure 1). An increasing amount of crystal material is observed at decreasing equilibrium temperatures below 55 °C (see Figure 7). The spectra at different temperatures shown in Figure 8 were taken at time intervals of a few minutes; i.e., the quench is much slower than that shown in Figure 1. During the quench there is no sign of a crystal phase at 48 and 45 °C, whereas it is clearly observed at these temperatures in equilibrium. However, Figure 1 shows that the liquid−solid transition has already occurred at these temperatures even during a faster quench. The implication is that the system crystallizes after the system has already jammed, and thus that it is not the crystallization that induces the liquid−solid transition. Nevertheless, the equilibrium fraction of crystalline material is formed relatively quickly (minutes rather than hours) except, probably, close to T_c where the shear modulus evolved very slowly.

Discussion

Given the small CAC, the volume fraction of the micelles is proportional to the polymer concentration: $\phi = v_sC$, where v_s is the specific volume of the micelles, i.e., the inverse of the so-called overlap concentration. v_s can be estimated from the weight-average molar mass, M_w, and z-average hydrodynamic radius, R_{hz}, of the micelles:

$$v_s = \frac{4\pi R_{hz}^3 N_a}{3M_w} \quad (1)$$

$M_w = 104$ kg/mol and $R_{hz} = 7.6$ nm almost independent of the temperature.[3] Using these values and neglecting the effect of polydispersity, we find $v_s = 1.0 \times 10^{-2}$ L/g. Alternatively, we can relate the measured intrinsic viscosity with that of equivalent hard spheres: $[\eta] = 2.5v_s$,[15] from which we derive $v_s = 6.2 \times 10^{-3}$ L/g at 20 °C. The two estimates of v_s are not equal because the micelles are not truly hard spheres.

In ref 3 it was shown that the concentration dependence of the osmotic compressibility at different temperatures can be described by the Carnahan−Stirling expression for noninteracting hard spheres at least up to 100 g/L.[16] However, the agreement was only obtained using an effective (thermodynamic) volume fraction (ϕ_{eff}) for the micelles that decreases with increasing temperature. The thermodynamic specific volume of the micelles decreases from 5.3×10^{-3} L/g at 20 °C to 2.8×10^{-3} L/g at 70 °C. In Figure 3, we show for comparison the polymer concentrations where ϕ_{eff} is unity. The comparison with the liquid−solid transition shows that the transition occurs roughly when ϕ_{eff} is unity. Earlier it was reported for other PEO-based polymeric micelles that the transition occurred at ϕ_{eff} somewhat smaller than unity.[17]

For a quantitative description of the structure factor we would need an expression for the form factor of the micelles. Castelleto et al.[4] observed that the expression for a homogeneous core with a corona of Gaussian chains gave a good description of the form factor of polymeric micelles with relatively short chains if one accounts for polydispersity. They assumed hard sphere interactions between the micelles to calculate the structure factor at finite concentrations. Very recently, Sommer et al. analyzed the structure factor of the same system we study here, at 20 g/L in terms of a radial volume profile and effective hard-sphere interactions.[18] These approaches were found to give a quantitative description of the structure factor at low concentrations, but they cannot be used if ϕ approaches or exceeds unity. At higher concentrations the PEO chains of different micelles start to overlap, and the softness of the interactions needs to be included.

In Figure 9, we superimposed the data in the high q range for a range of concentrations between 50 and 190 g/L, i.e., across the liquid−solid transition. The q-independent solvent scattering intensity was subtracted, but not the spurious upturn at the low-q end. The upturn at low q is caused by the finite width of the incident beam and was also observed for the solvent. It varies somewhat between measurements and cannot be subtracted without some ambiguity. The interaction peak at $q \approx 0.4$ nm^{-1} weakens because the scattering contrast of the PEO corona decreases if they more strongly overlap. However, the form factor of the hydrophobic core remains clearly visible and dominates for $q > 1$ nm^{-1}. The solid line in Figure 9 represents the form factor of a homogeneous sphere with a radius of 1.6 nm, which is close to that expected for a core containing 26 octadecane chains. We believe that, progressively, the system is better described in terms of small core particles in a semidilute solution of PEO. The interactions between the core particles are soft and long-range, which leads to a liquid order. A quantitative description of this situation would imply knowledge of

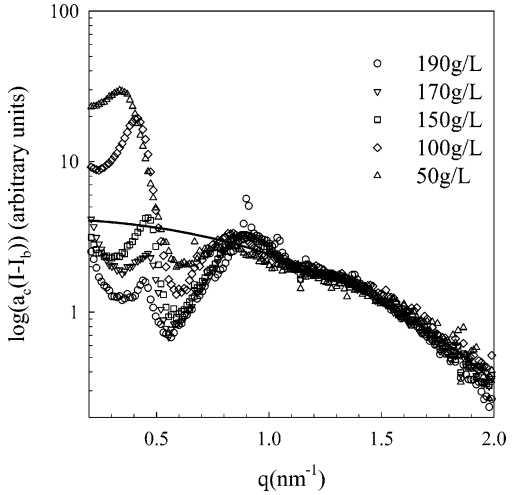

Figure 9. Superposition of the q dependence of the radial averaged scattering intensity at different concentrations (T = 28 °C) after subtraction of a q-independent baseline (I_b) and using vertical shift factors a_c. The solid line represents the form factor of a sphere with radius 1.6 nm.

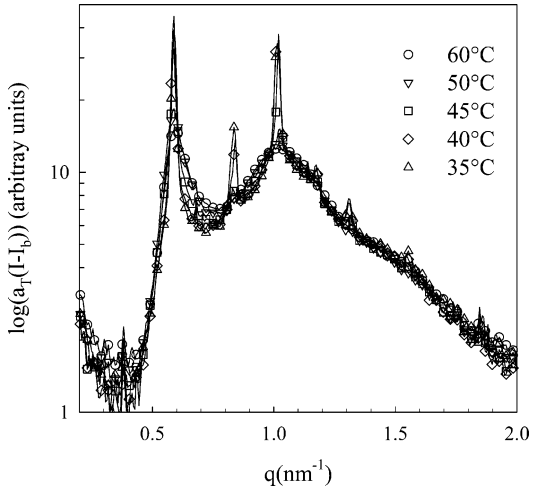

Figure 10. Superposition of the q dependence of the radial averaged scattering intensity at different temperatures (C = 300 g/L) after subtraction of a q-independent baseline (I_b) and using vertical shift factors a_T.

the concentration profile of the PEO chains around the cores and the pair correlation function of the cores in the solution.

At a specific concentration, which depends on the temperature, a crystal phase is formed, characterized by narrow Bragg peaks. Close to the critical concentration the crystal phase concerns only a small fraction of the micelles, and the scattering from micelles with liquid order dominates. Comparing the systems just before (170 g/L) and just after (190 g/L) shows that there is no dramatic change in the structure factor of the liquid phase with the appearance of the crystal phase. The fraction of crystalline material can be calculated by comparing the integrated intensity of the Bragg peaks with that of the whole system. From the data at 28 °C shown in Figure 7, we find <5, 13, 26, and 57% for 190, 225, 300, and 400 g/L, respectively.

For hard spheres the driving force for crystallization is the gain in translational entropy of the spheres.[19] For $\phi > 0.5$ a face-centered-cubic phase is formed in equilibrium with a liquid phase. The behavior of the polymeric micelles studied here is different from that of hard spheres not only because they are soft and can interpenetrate but also because the aggregation number, and thus the effective volume fraction of the micelles, can vary.

The formation of the crystal phase can be even better observed by varying the temperature at constant polymer concentration. In Figure 10, we show the data for C = 300 g/L at different temperatures after superposition in the high q range. It can be clearly seen that the liquid order is almost the same at each temperature and that the Bragg peaks simply appear on top of the liquid structure. It seems reasonable to assume that decreasing the temperature simply leads to an increase of the crystal phase without modifying the structure of the liquid phase.

Castelletto et al.[4] suggested that in so-called soft solids crystalline domains are formed in equilibrium with the liquid phase. The fraction of these domains increases with decreasing temperature. They found that the width of the first scattering peak decreased abruptly at the soft solid−solid transition which they interpreted as a transition from short-range crystal grains to a crystal with long-range order. It is not clear from ref 4 whether the fraction of the crystal phase becomes unity at the soft solid−solid transition. For the system studied here, we do not observe a soft solid−solid transition, and the first Bragg peak is very narrow as soon as it is observed. Clearly, the solid contains domains with long-range crystal order but nevertheless is not fully crystalline.

The viscosity of noninteracting hard spheres increases with increasing concentration and diverges at a critical volume fraction: $\phi_c \approx 0.6$. The concentration dependence can be well described by the equation $\eta = \eta_0(1 - C/C_c)^{-2}$.[20] For the present system this equation describes the viscosity up to about 70 g/L with $C_c \approx 110$ g/L at 20 °C; i.e., the critical volume fraction is 0.68 if we use the specific volume derived form the intrinsic viscosity. The effective thermodynamic volume fraction at this critical concentration is 0.58. For $C > 100$ g/L the viscosity has a power law dependence until the liquid−solid transition is reached at a viscosity of about 0.2 Pa s. It is not possible to obtain stable solutions with higher viscosities. However, as mentioned above, the viscosity of supercooled solutions obtained by very rapid quenches or extrapolation of the data obtained at higher temperatures follows the same power law concentration dependence as the equilibrium liquid systems at lower concentrations.

In monodisperse hard-sphere systems the viscosity is increased by a factor of about 50 over the solvent viscosity at the volume fraction were the crystalline phase appears ($\phi = 0.5$),[21] compared to about 200 for the present system. In hard-sphere systems the crystallization is slow, and systems can be quenched at higher volume fractions in a state with homogeneous liquid order sufficient long to determine the viscosity. In this way it is found that the viscosity increases continuously and diverges at the so-called glass transition $\phi \approx 0.6$, where the spheres are completely jammed. It is not yet established whether the slowly appearing crystal phase modifies the viscosity in this regime.

Polymeric micelles are soft and closely resemble star polymers with one important difference: the number of arms per micelle can vary. Star polymers with a large number of arms also show a liquid−solid transition as a function of temperature or concentration, but not

necessarily the formation of a crystal phase.[22] Diblock copolymer micelles in selective solvents usually have frozen cores and can thus be assimilated to star polymers if the core is small compared to the corona. These systems show a cubic crystal phase in the jammed state.[23−25] The viscosity of stars with a smaller number of arms does not diverge but has a power law concentration dependence above the overlap concentration.[26] This is what we observe for the micelles studied here in the stable or supercooled liquid phase.

The liquid−solid transition of the polymeric micelles studied here is discontinuous and is closely correlated with the appearance of a crystal phase. A continuous transition is observed for hard or soft spheres and star polymers. A systematic study of polymeric micelles formed by diblock copolymers with frozen cores also showed a continuous increase of the viscosity similarly to that of star polymers.[25] Therefore, we speculate that the discontinuous transition is caused by an increase of the number of arms per micelle. The concentration and temperature dependence of the viscosity in the liquid or supercooled state is the same as that of polymer stars with a constant relatively low number of arms, for which neither jamming nor crystallization is observed. Jamming and crystallization can only occur because the number of arms is much higher in the solid state. Unfortunately, we cannot calculate the aggregation number in the crystalline phase accurately because we do not know its volume fraction, but a rough estimate at the highest concentration gave an arm number of 100.

The liquid−solid transition occurs at the same viscosity independent of the concentration, and the temperature dependence in the liquid and supercooled state is the same at all concentrations. If there was an influence of the core on the interaction between micelles, the effect would become stronger with increasing concentration. The implication is that for the system studied here the core, which is much smaller than the corona, does not influence the interaction between the micelles.

The liquid−solid transition has the appearance of a thermodynamic phase transition that leads both to crystallization and jamming, although the fraction of crystalline material is very small just above the transition. Crystallization and jamming occur at the same temperature, but not at the same rate. During a temperature quench the system jams before crystalline material can be detected with SAXS, implying that crystallization is not the origin of jamming. Nevertheless, crystallization is relatively rapid because the interaction between stars is soft, and the systems can be quenched in the fully amorphous glassy state only for a very short time. It is clear that the elastic modulus of the system in the solid state is not caused by deformation of the lattice structure as was suggested for the case of diblock copolymer micelles.

Summary

Polymeric micelles based on hydrophobically end-capped PEO in water show a discontinuous liquid−solid transition with decreasing temperature or increasing concentration. A a liquid crystalline body-centered-cubic phase is formed in the solid with a weight fraction that increases with increasing concentration or decreasing temperature, but which is less than 5% at the transition. When decreasing the temperature, the bcc phase is formed relatively quickly, but only after the system has jammed. In the liquid state the micelles behave like polymeric stars with a constant low arm number, but in the solid state the arm number is much increased. The discontinuous liquid−solid transition is perhaps a thermodynamic phase transition, which leads to both jamming and crystallization.

The initial concentration dependence of the osmotic modulus can be described in terms of hard spheres with an effective volume. The liquid−solid transition occurs when the effective volume fraction of the micelles is about unity. The viscosity at the threshold is about 0.2 Pa s independent of the polymer concentration. The transition is generally rapid but is very slow very close to the threshold. The shear modulus of the solid phase increases weakly with increasing concentration and decreasing temperature.

Acknowledgment. This work has been supported in part by a grant from the Marie Curie Program of the European Union numbered MRTN-CT-2003-504712.

References and Notes

(1) Hamley, I. W. *The Physics of Block Copolymers;* Oxford University Press: Oxford, 1998.
(2) Lobry, L.; Micali, N.; Mallamace, F.; Liao, C.; Chen, S. H. *Phys. Rev. E* **1999**, *60*, 7076.
(3) Lafleche, F.; Durand, D.; Nicolai, T. *Macromolecules* **2003**, *36*, 1331.
(4) Castelletto, V.; Caillet, C.; Fundin, J.; Hamley, I. W. *J. Chem. Phys.* **2002**, *116*, 10947.
(5) Kaczmarski, J. P.; Glass, J. E. *Macromolecules* **1993**, *26*, 5149.
(6) Yekta, A.; Xu, B.; Duhamel, J.; Adiwidjaja, H.; Winnik, M. A. *Macromolecules* **1995**, *28*, 956.
(7) Annable, T.; Buscall, R.; Ettelai, R.; Whittlestone, D. *J. Rheol.* **1993**, *37*, 695.
(8) Alami, E.; Rawiso, M.; Isel, F.; Beinert, G.; Binane-Limbele, W.; François, J. *ACS Adv. Chem.* **1996**, *248*, 343.
(9) François, J.; Maitre, S.; Rawiso, M.; Sarazin, D.; Beinert, G.; Isel, F. *Colloids Surf. A* **1996**, *112*, 251.
(10) Abrahamsén-Alami, S.; Alami, E.; François, J. *J. Colloid Interface Sci.* **1996**, *179*, 20.
(11) Alami, E.; Almgren, M.; Brown, W. *Macromolecules* **1996**, *29*, 5026.
(12) Chassenieux, C.; Nicolai, T.; Durand, D. *Macromolecules* **1997**, *30*, 4952.
(13) Séréro, Y.; Aznar, R.; Porte, G.; Berret, J. F.; Calvet, D.; Collet, A.; Viguier, M. *Phys. Rev. Lett.* **1998**, *81*, 5584.
(14) Pham, Q. T.; Russel, W. B.; Thibeault, J. C.; Lau, W. *Macromolecules* **1999**, *32*, 2996.
(15) Russel, W. B.; Saville, D. A.; Schowalker, W. R. *Colloidal Dispersions*; Cambridge University Press: Cambridge, 1989.
(16) Hansen, J. P.; McDonald, I. R. *Theory of Simple Liquids*; Academic Press: San Diego, 1990.
(17) Yang, Z.; Pousia, E.; Nixon, S. K.; Price, C.; Booth, C.; Hamley, I. A.; Castelletto, V.; Fundin, J. *Langmuir* **2001**, *17*, 8085.
(18) Sommer, C.; Pederson, J. S. *Macromolecules* **2004**, *37*, 1682.
(19) For exemple: Frenkel, D. In *Soft and Fragile Matter*; Cates, M., Evans, M., Eds.; Institute of Physics Publishing: Bristol, UK, 2000; pp 113−144.
(20) Berli, C. L. A.; Quemada, D. *Langmuir* **2000**, *16*, 7968.
(21) Meeker, S. P.; Poon, W. C. K.; Pusey, P. N. *Phys. Rev. E* **1997**, *55*, 5718.
(22) Loppinet, B.; Stiakakis, E.; Vlassopoulos, D.; Fytas, G.; Roovers, J. *Macromolecules* **2001**, *34*, 8216.
(23) Watanabe, H.; Kotado, T.; Hashimoto, T.; Shibayama, M.; Kawai, H. *J. Rheol.* **1982**, *26*, 153.
(24) Gast, P. *Langmuir* **1996**, *12*, 4060.
(25) Buitenhuis, J.; Förster, S. *J. Chem. Phys.* **1997**, *107*, 262.
(26) Roovers, J. *Macromolecules* **1994**, *27*, 5359.

MA049101Y